Supporting Information

Ultrafast Electron and Hole Relaxation Pathways in Few-Layer MoS_2

Zhaogang Nie,[a] Run Long,[b,c,d] Jefri S. Teguh,[a] Chung-Che Huang,[e] Daniel W. Hewak,[e] Edwin K. L. Yeow,[a] Zexiang Shen,[f,g,h] Oleg V. Prezhdo,[b] and Zhi-Heng Loh[a,f*]*

[a] Division of Chemistry and Biological Chemistry, School of Physical and Mathematical Sciences, Nanyang Technological University, Singapore 637371, Singapore

[b] Department of Chemistry, University of Southern California, Los Angeles, California 90089, United States

[c] School of Physics, Complex Adaptive Systems Laboratory, University College Dublin, Belfield, Dublin 4, Ireland

[d] College of Chemistry, Key Laboratory of Theoretical & Computational Photochemistry of Ministry of Education, Beijing Normal University, Beijing, 100875, P. R. China.

[e] Optoelectronics Research Centre, University of Southampton, Southampton SO17 1BJ, United Kingdom

[f] Division of Physics and Applied Physics, School of Physical and Mathematical Sciences, Nanyang Technological University, Singapore 637371, Singapore

[g] Centre for Disruptive Photonic Technologies, School of Physical and Mathematical Sciences, Nanyang Technological University, Singapore 637371, Singapore

[h] Division of Materials Technology, School of Materials Science and Engineering, Nanyang Technological University, Singapore 639798, Singapore

[*] Corresponding Authors: (O.V.P.) E-mail: prezhdo@usc.edu. Telephone: +1 (213) 821-3116. (Z.-H.L.) E-mail: zhiheng@ntu.edu.sg. Telephone: +65 6592-1655.

1. Fit Parameters for Intravalley Electronic Relaxation Dynamics

The temporal evolution of the spectral first moment $\langle\lambda^{(1)}(t)\rangle$ computed about the exciton B transition is fit to a Gaussian decay function of the form

$$\langle\lambda^{(1)}(t)\rangle = \Delta\lambda\, e^{-t^2/2\left(\tau_e^{(1)}\right)^2} + \lambda_0 \tag{S1}$$

where $\Delta\lambda$ is the amplitude of the blueshift, $\tau_e^{(1)}$ is the Gaussian decay time, and λ_0 is the offset wavelength. The fit parameters are summarized in Table S1 below.

Table S1. Fit parameters extracted from $\langle\lambda^{(1)}(t)\rangle$.

Fluence (mJ/cm^2)	$\boldsymbol{\Delta\lambda}$ **(nm)**	$\boldsymbol{\tau_e^{(1)}}$ **(ps)**	$\boldsymbol{\lambda_0}$ **(nm)**
0.06	21.4 ± 0.7	1.77 ± 0.08	602.2 ± 0.6
0.14	20.9 ± 0.2	1.34 ± 0.02	602.4 ± 0.1
0.29	13.3 ± 0.1	1.34 ± 0.02	610.4 ± 0.1

From the above, it is seen that the offset wavelength λ_0 increases with excitation fluence. This trend is consistent with increased band gap renormalization at larger carrier densities, resulting in a decrease in the band gap with increasing carrier density.

2. Calculation of the Excess Energies of the Carriers

The excess energies of the carriers are calculated by first determining the threshold wavelength for the direct-gap optical absorption at the K valley. The threshold wavelength is ascertained to be 759 nm from the linear fits to the baseline and the absorption peak (Figure S1). Given that the absorption maximum of the exciton A transition resides at 684 nm, the total excess energy of the carriers is therefore 1440 cm^{-1}. By employing the m_e^*/m_h^* ratio of 1.76 obtained from first-principles electronic structure calculations,[1] the excess energies of the

electron and hole are calculated to be 620 ± 230 and 820 ± 290 cm^{-1}, respectively. The relatively large error margins arise from the presence of an exponentially decaying absorption feature in the long wavelength region that is due to indirect transitions. This long-wavelength absorption tail introduces uncertainty in determining the appearance threshold of the absorption peak.

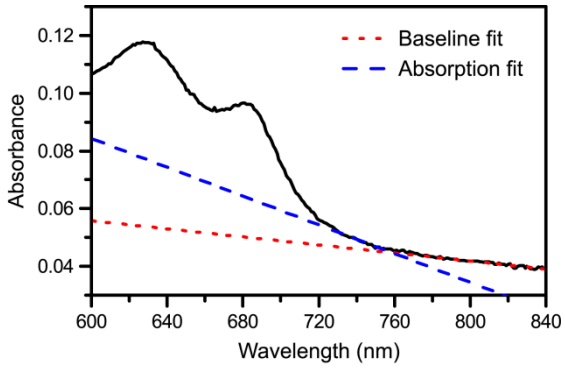

Figure S1. Determination of the threshold wavelength for the direct-gap optical absorption of the five-layer MoS_2 sample. The optical absorption spectrum acquired at 300 K is shown as the solid line. The threshold wavelength is given by the intersection between the linear fits to the baseline (dotted line) and to the absorption peak (dashed line).

3. Reconstructed transmission spectrum of the pure photoexcited sample

The differential transmission signal $\Delta T/T$ is directly obtained by measuring the transmitted intensity of the probe with (I_{on}) and without (I_{off}) the pump beam. That is,

$$\Delta T/T = \left(I_{on} - I_{off}\right)/I_{off}. \quad \text{(S1)}$$

To reconstruct the transmission spectrum of the pure photoexcited species T_e, one requires knowledge of the excitation fraction f and the intensity of the probe beam before the sample (I_0). While the former can be determined, the latter is not usually measured in the experiments.

Nevertheless, T_e can be reconstructed from the measured $\Delta T/T$ spectrum and an independently measured ground-state sample transmission spectrum T by employing the expression

$$T_e = T\left(\frac{\Delta T}{T} + 1\right)^{1/f}. \quad \text{(S2)}$$

The above procedure is used to reconstruct the transmission spectrum of the pure photoexcited species that is produced by the excitation of five-layer MoS_2 sample at 300 K with a pump fluence of 0.29 mJ/cm^2 (see Fig. 6c of the main text). The resultant transmission spectrum is dominated by a $T_e > 1$ feature (Fig. S2), which is consistent with probe pulse-induced stimulated emission. However, it is important to note that the absolute value of T_e is highly sensitive to the excitation fraction f, which itself is challenging to quantify accurately. The T_e spectrum should therefore be analyzed only qualitatively.

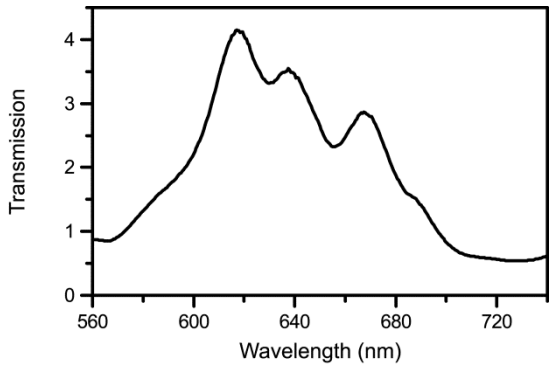

Figure S2. Reconstructed transmission spectrum of the pure photoexcited species at a time delay of 200 fs following excitation of the five-layer MoS_2 sample at 300 K with a pump fluence of 0.29 mJ/cm^2.

4. Resonant Raman Spectrum of Five-Layer MoS_2

The resonant Raman spectrum of the five-layer MoS_2 sample is recorded at 295 K on a Horiba LabRAM HR instrument with 632.8-nm irradiation. The Raman spectrum and its second derivative spectrum are shown in Figure S3.

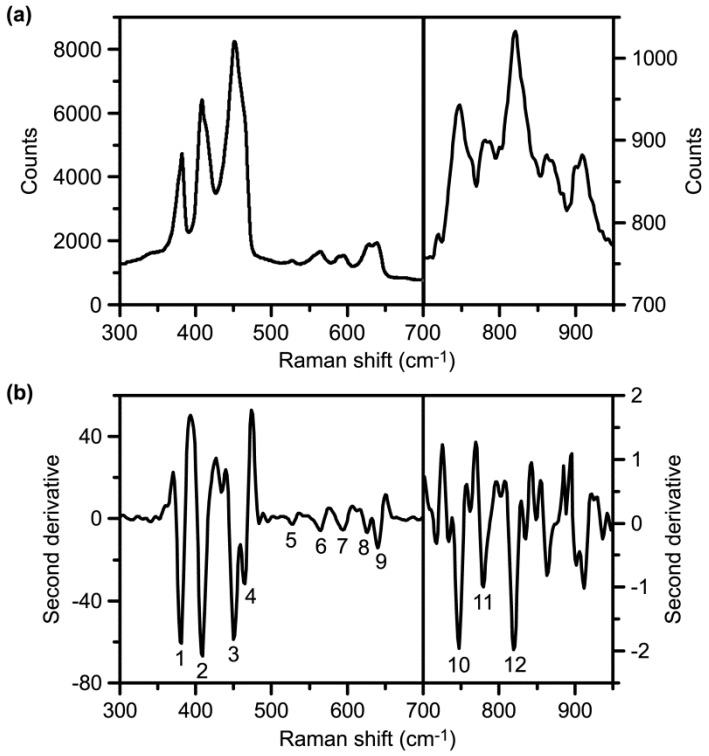

Figure S3. (a) Resonant Raman spectrum for the five-layer MoS_2 sample and (b) its second-derivative spectrum.

The labeled peaks in the second-derivative spectrum are assigned according to previous reports in the literature.[2–4] The assignment is given in Table S2 below.

Table S2. Assignment of peaks observed in the resonant Raman spectrum of five-layer MoS_2. The peak numbers are used to identify the negative-valued minima observed in the second-derivative spectrum (Figure S2b).

Peak No.	Frequency (cm^{-1})	Assignment
1	381	$E^1_{2g}(\Gamma)$
2	409	$A_{1g}(\Gamma)$
3	450	$2LA(M)$
4	465	$A_{2u}(\Gamma)$
5	528	$E_{1g}(M) + LA(M)$
6	565	$2E_{1g}(\Gamma)$
7	594	$E^1_{2g}(\Gamma) + LA(M)$
8	626	unknown
9	640	$A_{1g}(M) + LA(M)$
10	747	$2E^1_{2g}(M)$
11	779	$A_{1g}(M) + E^1_{2g}(M)$
12	819	$2A_{1g}(\Gamma)$ or $2A_{1g}(M)$

The unknown peak at 626 cm^{-1} was also observed in earlier resonant Raman measurements of few-layer MoS_2 samples,[4] although its origin remains unknown.

5. Measured Optical Pump-Probe Cross-Correlation

The time resolution of the experimental apparatus is measured by performing a second-order pump-probe intensity cross-correlation with a 10-μm-thick BBO crystal located at the sample position. The resultant cross-correlation trace yields a full-width at half-maximum (FWHM) of 83 fs (Figure S4).

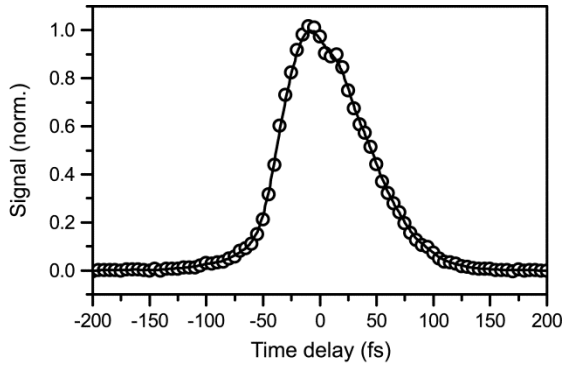

Figure S4. Cross-correlation trace of the pump and probe pulses. The FWHM is 83 fs.

6. Pump Fluence-Dependence Measurements

Pump fluence-dependence measurements were performed to verify that photoexcitation of the sample occurs in the linear regime. Figure S5 shows a log-log plot of the peak $\Delta T/T$ signal S obtained at the B exciton transition as a function of fluence F. Because $S \propto F^N$, the slope of the log-log plot yields the photon order N, which in this case is found to be 1.05 ± 0.06. This result confirms that excitation of the MoS_2 sample under our experimental conditions occurs in the linear regime.

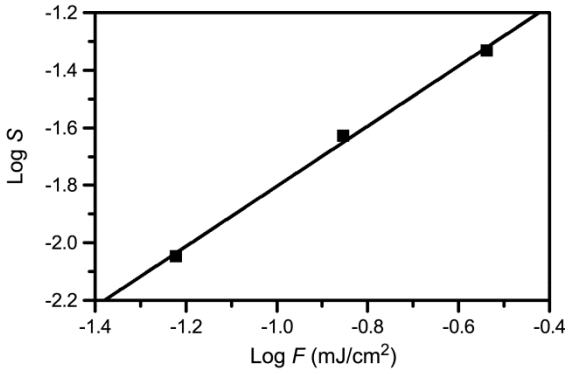

Figure S5. Dependence of the maximum $\Delta T/T$ signal on the pump fluence, confirming one-photon excitation of the sample.

References

1. Qiu, D. Y.; da Jornada, F. H.; Louie, S. G. Optical Spectrum of MoS_2: Many-Body Effects and Diversity of Exciton States. *Phys. Rev. Lett*. **2013**, *111*, 216805.
2. Chen, J. M.; Wang, C. S. Second Order Raman Spectrum of MoS_2. *Solid State Commun*. **1974**, *14*, 857–860.
3. Stacy, A. M.; Hodul, D. T. Raman Spectra of IVB and VIB Transition Metal Disulfides Using Laser Energies Near the Absorption Edges. *J. Phys. Chem. Solids* **1985**, *46*, 405–409.
4. Chakraborty, B.; Ramakrishna Matte, H. S. S.; Sood, A. K.; Rao, C. N. R. Layer-Dependent Resonant Raman Scattering of a Few Layer MoS_2. *J. Raman Spectrosc*. **2013**, *44*, 92–96.